Environmental Science & Technology

pubs.acs.org/est

Article

Metabolomic Responses of Green Alga *Chlamydomonas reinhardtii* Exposed to Sublethal Concentrations of Inorganic and Methylmercury

Vera I. Slaveykova,* Sanghamitra Majumdar, Nicole Regier, Weiwei Li, and Arturo A. Keller

Cite This: *Environ. Sci. Technol.* 2021, 55, 3876−3887

Read Online

ACCESS | Metrics & More | Article Recommendations | Supporting Information

ABSTRACT: Metabolomics characterizes low-molecular-weight molecules involved in different biochemical reactions and provides an integrated assessment of the physiological state of an organism. By using liquid chromatography−mass spectrometry targeted metabolomics, we examined the response of green alga *Chlamydomonas reinhardtii* to sublethal concentrations of inorganic mercury (IHg) and monomethylmercury (MeHg). We quantified the changes in the levels of 93 metabolites preselected based on the disturbed metabolic pathways obtained in a previous transcriptomics study. Metabolites are downstream products of the gene transcription; hence, metabolite quantification provided information about the biochemical status of the algal cells exposed to Hg compounds. The results showed that the alga adjusts its metabolism during 2 h exposure to 5×10^{-9} and 5×10^{-8} mol L^{-1} IHg and MeHg by increasing the level of various metabolites involved in amino acid and nucleotide metabolism, photorespiration, and tricarboxylic acid (TCA) cycle, as well as the metabolism of fatty acids, carbohydrates, and antioxidants. Most of the metabolic perturbations in the alga were common for IHg and MeHg treatments. However, the exposure to IHg resulted in more pronounced perturbations in the fatty acid and TCA metabolism as compared with the exposure to MeHg. The observed metabolic perturbations were generally consistent with our previously published transcriptomics results for *C. reinhardtii* exposed to the comparable level of IHg and MeHg. The results highlight the potential of metabolomics for toxicity evaluation, especially to detect effects at an early stage of exposure prior to their physiological appearance.

INTRODUCTION

Advances in "omic" technologies have opened novel avenues in ecotoxicology research toward elucidating contaminant modes of action, biomarker discovery, and predictive risk assess- ment.[1,2] Metabolomics, the youngest among the "omic" technologies, characterizes low-molecular-weight metabolites involved in different biochemical reactions and captures the cellular status and physiological state of an organism.[3−6] Existing advancements in environmental metabolomics, in particular chemical stressor-induced metabolic perturbations in different organisms, including fish, invertebrates,[7,8] plants,[9,10] and microalgae,[11] were comprehensively reviewed. However, relatively few studies have explored contaminant-induced metabolic perturbations in phytoplanktons to address ecotoxicological questions. In the specific case of toxic metals, such as Ag, Cd, Cu, Pb, and Zn, only a few metabolomic studies with green algae, diatoms, or cyanobacteria have been carried out.[6,11−13] Based on a literature search (keywords: mercury, metabolomics, and algae), no studies exist that deal with the metabolomics response of algae exposed to Hg, a priority contaminant of global importance.

The present study focusses on Hg as characterized with high persistence and bioaccumulative and biomagnifying poten- tial.[14] The toxicity of Hg toward living beings is well-known;[15] however, the metabolomic response is not well-understood. There has been progress in the overall understanding of the adverse effects of Hg, including at the molecular level, with comprehensive reviews for animal cells, invertebrates and vertebrates,[16] phytoplanktons,[17,18] and aquatic plants.[19,20] However, these previous studies focused on distinct effects or do not cover the level of resolution we are considering in this study. The physiological and transcriptomic responses in green alga *Chlamydomonas reinhardtii* during short-term exposure to inorganic mercury (IHg) and monomethylmercury (CH_3Hg^+ and MeHg), two mercury species prevailing in the

Received: December 14, 2020
Revised: February 12, 2021
Accepted: February 16, 2021
Published: February 25, 2021

https://dx.doi.org/10.1021/acs.est.0c08416

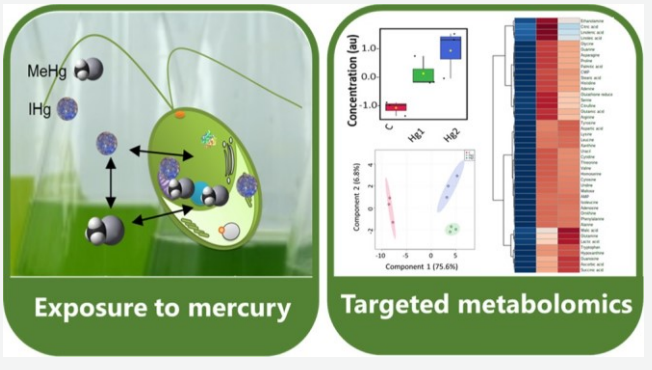

aquatic environments, were assessed.[21−23] These studies demonstrated that multiple metabolic pathways could be disturbed by IHg and MeHg, including those related to dysregulation of antioxidants, detoxification, energy resources, and so forth.[21−23] However, transcriptomics provides only a partial understanding of the cellular response, given that not all genes that are transcribed are translated into functional gene products.[24] As downstream products of the gene transcription and protein expression, metabolites provide information about the biochemical status of the algal cells exposed to Hg compounds.

In such a context, the primary goal of the present study was to further examine the responses of the green alga *C. reinhardtii* to sublethal concentrations of IHg and MeHg by using targeted metabolomics in order to obtain novel insights into the molecular basis underlying the cellular responses to mercury compounds. Liquid chromatography−mass spectrometry (LC−MS) targeted metabolomics was employed to quantify over 93 metabolites preselected based on the disturbed metabolic pathways determined by transcriptom- ics.[22] Targeted metabolomics was chosen as it provides the advantage of more sensitive and accurate detection of predetermined metabolites.[25] The metabolomics results were compared with the physiological responses and the tran- scriptomics study from our previous work.[22]

MATERIAL AND METHODS

Chemicals and Labware. All the labware material was pre-washed in 10% HNO_3 (EMSURE, Merck, Darmstadt, Germany), followed by a 10% HCl acid bath (EMSURE, Merck, Darmstadt, Germany) for 2 h under sonication, thoroughly rinsed with ultrapure water (Milli-Q direct system, Merck, Darmstadt, Germany), and subsequently autoclaved for sterilization. $HgCl_2$ (IHg) and CH_3HgCl (MeHg) standard solutions (1.0 g L^{-1}) were purchased from Sigma-Aldrich, Buchs, Switzerland.

Culture Conditions and Exposure to Mercury Compounds. The green alga *C. reinhardtii* CPCC11 (Canadian Phycological Culture Centre, Waterloo, Canada) was axeni- cally grown in 4× diluted Tris-acetate-phosphate medium[26] at 20.2 ± 0.5 °C, 115 rpm, and 12:12 h light/dark cycle in a specialized incubator (Multitron Infors HT, Bottmingen, Switzerland). At the mid-exponential growth phase, the algal cultures were isolated from the growth medium by gentle centrifugation (4 °C, 10 min, 1300*g*), rinsed, and re-suspended in the exposure medium. The exposure medium contained 8.2 × 10^{-4} mol L^{-1} $CaCl_2 \cdot 2H_2O$, 3.6 × 10^{-4} mol L^{-1} $MgSO_4 \cdot 7H_2O$, 2.8 × 10^{-4} mol L^{-1} $NaHCO_3$, 1.0 × 10^{-4} mol L^{-1} KH_2PO_4, and 5.0 × 10^{-6} mol L^{-1} NH_4NO_3, adjusted to pH 7.0 ± 0.1. Given the dependence of the algal metabolic state on the growth phase[27] and the light and dark cycle,[28] the experiments were performed with cells sampled exactly at the same growth stage (68 h), 4 h after the light in the incubator was switched on. For each test, the algal cells were re- suspended in the exposure medium to a final density of 4 × 10^6 cells·mL^{-1} in the absence (unexposed control, C) and presence of IHg or MeHg with a nominal concentration of 5 × 10^{-9} (IHg1) or 5 × 10^{-8} mol L^{-1} (IHg2) of IHg or 5 × 10^{-9} mol L^{-1} (MeHg1) or 5 × 10^{-8} mol L^{-1} (MeHg2) of MeHg. Cell density was determined using a Coulter counter (Beckman Coulter Counter).

To enable comparison with the already published transcriptomics and physiological effects results,[22] an exposure duration of 2 h was selected. Exposures and analyses were performed on three independent biological replicates. At the end of the exposure period, the microorganisms were centrifuged for 10 min at 1300*g*. The supernatant was discarded and the pellet deployed in liquid nitrogen to stop the metabolic activities. The pellets were kept at −80 °C overnight and then freeze-dried (Beta 1-8K, Christ, Germany). **Determination of Mercury Concentrations in the Exposure Medium and Algal Cells.** The cellular concen-tration of total mercury (THg = IHg + MeHg) in *C. reinhardtii* was determined from the freeze-dried pellets by atomic absorption spectrometry using a direct mercury analyzer DMA-80 (Milestone, USA). The accuracy of the measure-ments was evaluated by following the certified reference material (CRM) MESS-3 from the National Research Council of Canada, showing 100 ± 0.1% recovery. The amount of THg accumulated by algal cells was expressed in mg kg^{-1} dry weight of algal biomass (Figure S1, Supporting Information). The concentrations of THg in the exposure medium were measured by using a MERX automated total mercury analytical system (Brooks Rand Instruments, Seattle, WA, USA), with a detection limit of 1.5 × 10^{-13} mol L^{-1}. The accuracy of THg measurements by MERX was tested by analyzing the CRM ORMS-5 (National Research Council of Canada, 116.0 ± 3.5% recovery). The measured concentrations of IHg in the exposure medium corresponding to the nominal concen-trations of 5 × 10^{-9} and 5 × 10^{-8} mol L^{-1} were (1.55 ± 0.01) × 10^{-9} and (6.70 ± 0.60) × 10^{-8} mol L^{-1}, respectively. For nominal concentrations of 5 × 10^{-9} and 5 × 10^{-8} M MeHg, the measured concentrations were (3.70 ± 0.21) × 10^{-9} and

https://dx.doi.org/10.1021/acs.est.0c08416

$(6.59 \pm 0.23) \times 10^{-8}$ mol L^{-1}, respectively.

All the results are reported as mean and standard deviation, calculated from three independent experiments. One-way analysis of variance (ANOVA) was performed to test for significant differences between the treatments by the statistical module built in SigmaPlot 12.5 (Systat Software, CA, USA). The Tukey honestly significant difference test was performed as a post-hoc test. A $p < 0.05$ was considered statistically significant.

LC−MS-Based Targeted Metabolomics. The metabolic alterations in the green alga *C. reinhardtii* exposed to IHg or MeHg were determined by LC−MS-based targeted metab- olomics using an Agilent 6470 liquid chromatography triple quadrupole mass spectrometer (Agilent Technologies, USA) as previously described.[29−31] Ninety-three metabolites, including antioxidants, amines, amino acids, organic acids/phenolics, nucleobases/-sides/-tides, sugar/sugar alcohols, and fatty acids, were extracted following the previously developed method-ology.[13,29,30] The list of considered metabolites was the same as in our previous study[13] and is provided in Table S1 together with their measured limits of detection (MDLs).

Statistical and pathway analyses of the metabolomics data were performed for controls and IHg and MeHg exposures using MetaboAnalyst 4.0.[32,33] First, the data were corrected for the batch effect using the built-in module for MetaboAnalyst, based on the ComBat method.[34] Next, one-way ANOVA followed by Fisher's LSD post-hoc analysis with a $p < 0.05$ was completed to screen for metabolites differing in concentrations between Hg treatments and controls. Unsupervised principal component analysis (PCA) and supervised partial least squares-discriminant analysis (PLS-DA) were performed to get a global overview of the metabolic changes. Metabolites with a variable importance in the projection (VIP) greater than

https://dx.doi.org/10.1021/acs.est.0c08416

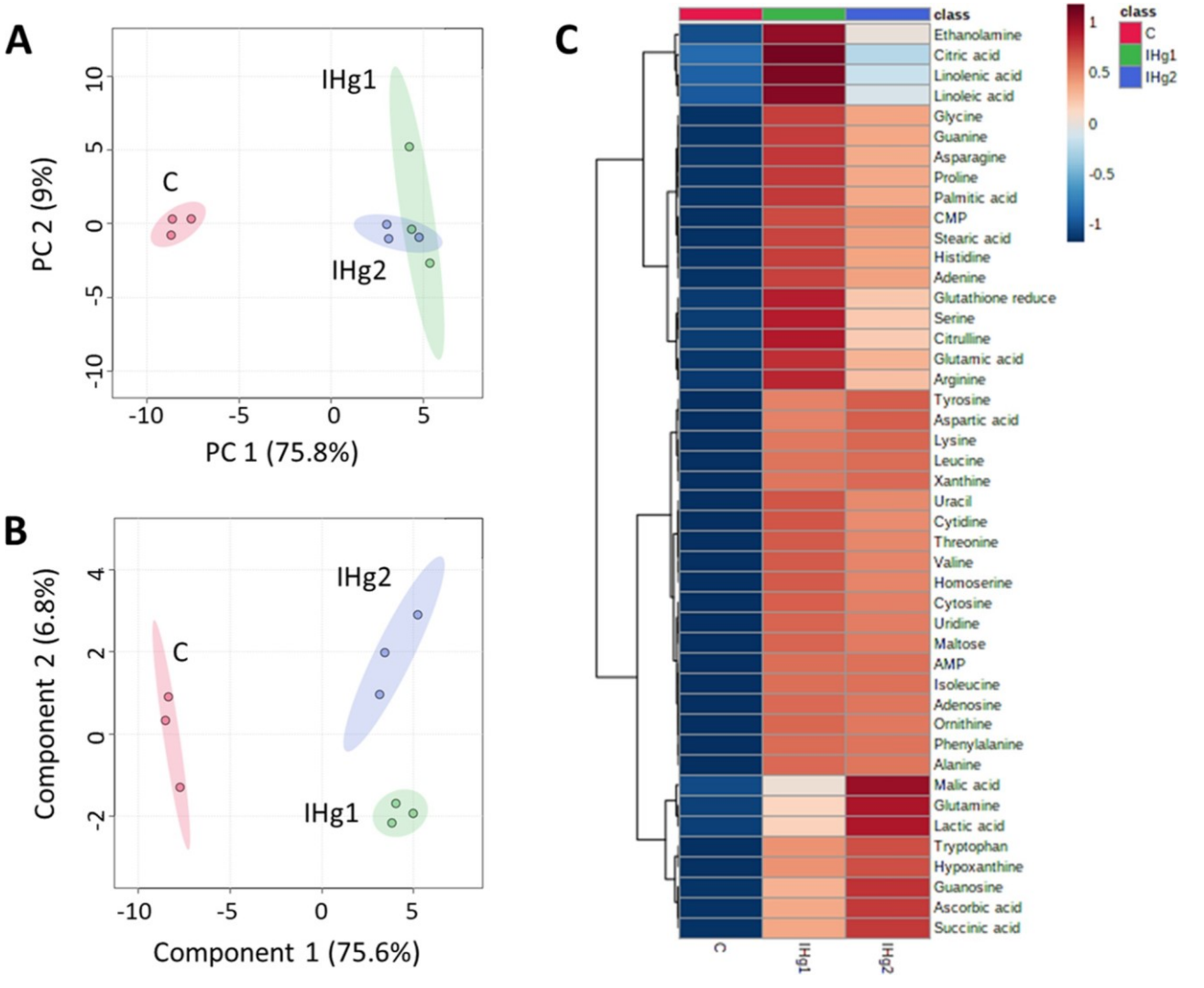

Figure 1. Analysis of the metabolic response of *C. reinhardtii* treated for 2 h with 5×10^{-9} mol L^{-1} IHg (IHg1) and 5×10^{-8} mol L^{-1} IHg (IHg2):
(A) PCA and (B) PLS-DA score plots. (C) Clustering metabolites and samples shown in a heat map (Euclidean distance and Ward clusteringalgorithm). Data were not normalized or transformed but were autoscaled.

1 were regarded as signi*fi*cant and responsible for group separation.[35] Metabolite concentrations were not subjected to any further normalization or transformation.

Metabolites signi*fi*cantly dysregulated by the respective Hg treatments, as identi*fi*ed via ANOVA and PLS-DA, were further considered in the pathway analysis to identify the most relevant pathways altered by sublethal levels of IHg or MeHg. Pathway enrichment and pathway topology analyses were performed with MetaboAnalyst 4.0[32,33] with respect to the KEGG pathway built-in metabolic library of the green alga *Chlorella variabilis*.[33] Over-representation analysis was per- formed using Fisher's exact test. The pathway topology analysis uses the node centrality measure to estimate that the node importance was "betweenness centrality". Pathways with threshold >0.1 were considered as signi*fi*cantly dysregulated.[32,36]

RESULTS AND DISCUSSION

Overview of Metabolic Profiles in *C. reinhardtii* Exposed to IHg and MeHg. Of a total of 93 metabolites analyzed, 52 were detected above their MDLs (Table S1) and quanti*fi*ed in the controls and IHg and MeHg treatments. A

https://dx.doi.org/10.1021/acs.est.0c08416

general overview of the treatment clustering was obtained by the unsupervised PCA and supervised PLS-DA methods. The PCA and PLS-DA score plots for IHg (Figure 1) and MeHg (Figure 2) treatments showed a good separation between the Hg treatments and the untreated control. Based on a VIP score >1, 30 responsive metabolites were subsequently employed to distinguish the untreated controls from IHg treatments (Figure S2). After comparing the IHg treatments to the untreated control by ANOVA, 15 additional metabolites were identified as significantly dysregulated (Table S2). All the 45 responsive metabolites were upregulated by Hg treatments in comparison with that in the untreated control (Figure 1C); however, the intensity of the dysregulation was concentration-dependent. For the MeHg treatments, a total of 39 responsive metabolites were identified via the VIP score and ANOVA, after comparison to the untreated controls (Figures 2C and S3, Table S3). All of them had increased levels upon MeHg treatments as compared with that in the untreated control, but the relative metabolite abundance was dose-dependent.

Heatmap clustering served to group the quantified responsive metabolites (Figures 1C and 2C). Globally, three large groups were obtained. Group 1 corresponded to

https://dx.doi.org/10.1021/acs.est.0c08416

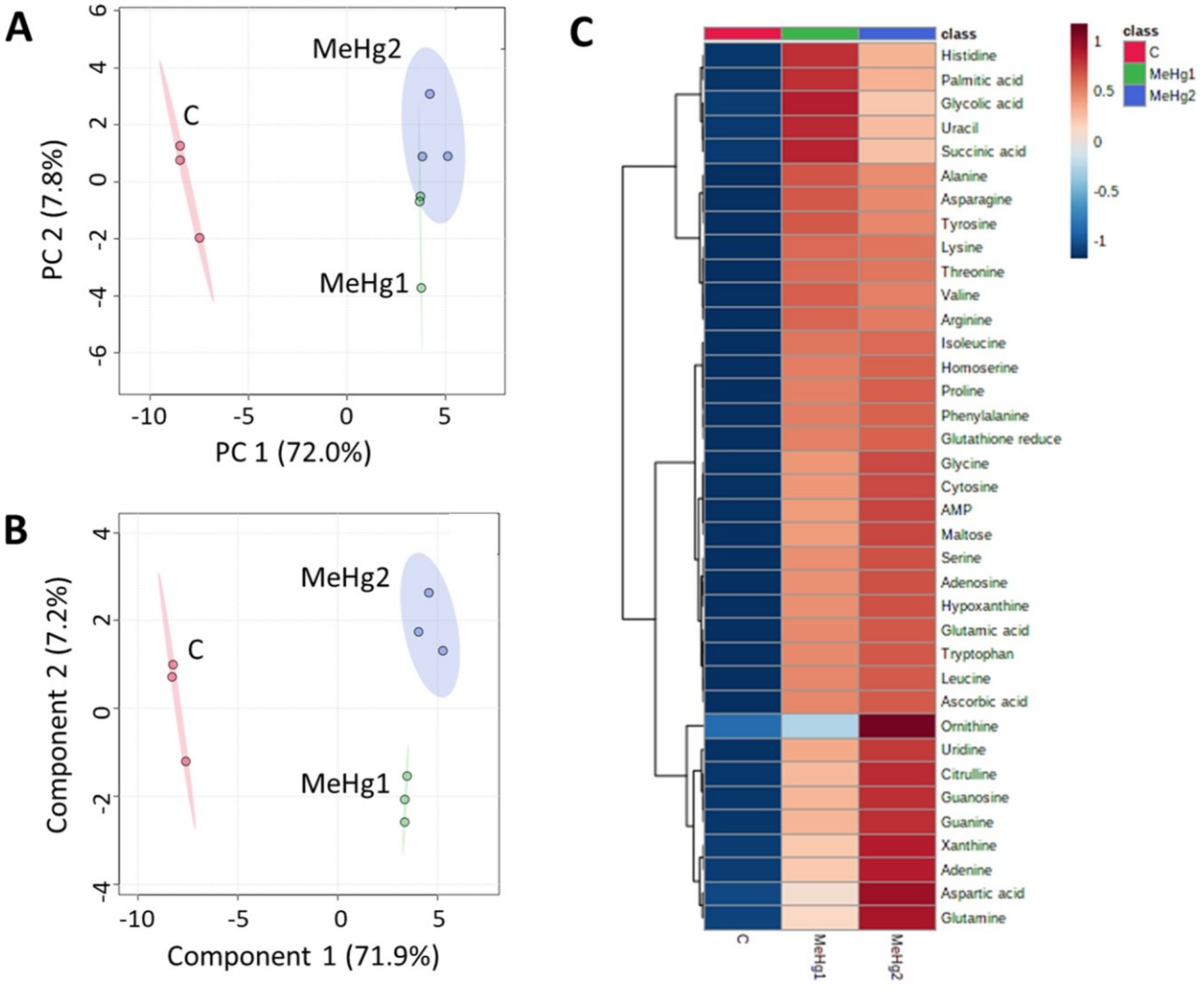

Figure 2. Analysis of the metabolic response of *C. reinhardtii* treated for 2 h with 5×10^{-9} mol L^{-1} MeHg (MeHg1), 5×10^{-8} mol L^{-1} MeHg (MeHg2); unexposed control (C). (A) PCA, (B) PLS-DA score plots. (C) Clustering metabolites and samples shown in a heat map (Euclidean distance and Ward clustering algorithm). Data were not normalized or transformed, but were autoscaled.

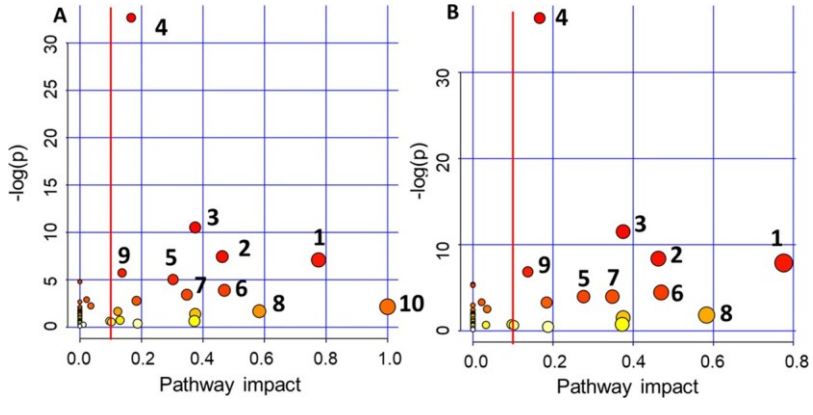

Figure 3. Pathway analysis for metabolites with the altered abundance in *C. reinhardtii* exposed to (A) IHg and (B) MeHg. The node color is based on its *p*-value and changes from red to yellow with the increase of the *p*-value. The node size reflects the pathway impact values, with bigger nodes corresponding to high impact values. Affected pathways: (1) alanine, aspartate, and glutamate metabolism, (2) glycine, serine, and threonine metabolism, (3) arginine biosynthesis, (4) aminoacyl-tRNA biosynthesis, (5) glyoxylate and dicarboxylate metabolism, (6) glutathione metabolism,
(7) arginine and proline metabolism. (8) Isoquinoline alkaloid biosynthesis, (9) purine metabolism; and (10) linoleic acid metabolism. A total of 45 responsive metabolites for IHg and 39 for MeHg obtained in algal treatments with 5×10^{-9} and 5×10^{-8} mol L^{-1} IHg or MeHg were used forthe pathway analysis.

https://dx.doi.org/10.1021/acs.est.0c08416

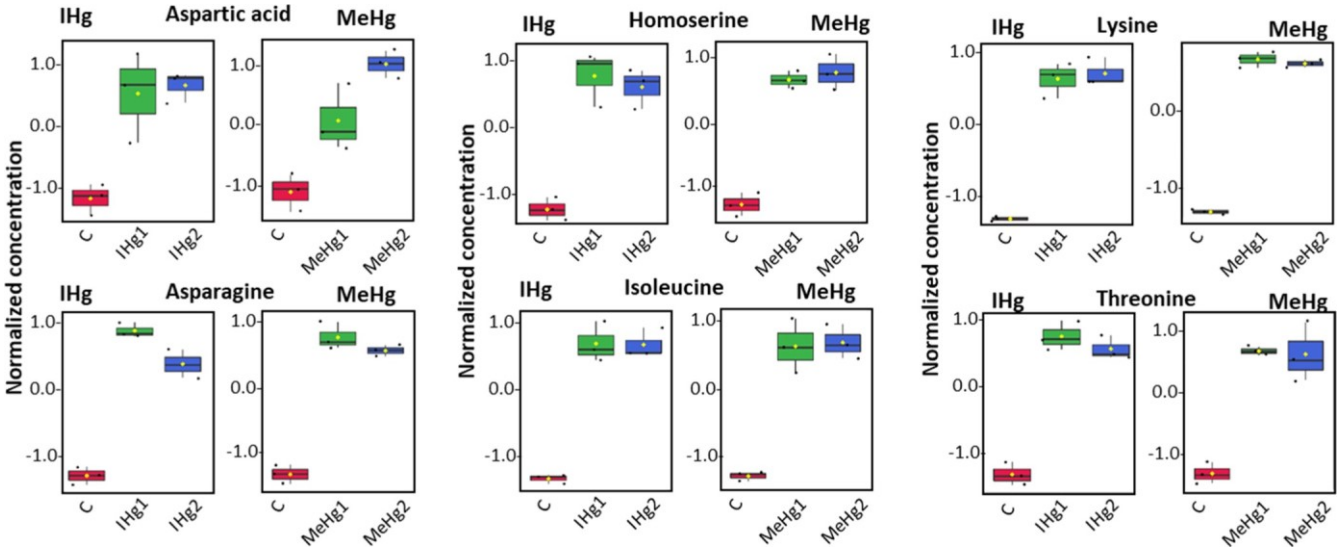

Figure 4. Box plots of relative abundance of oxaloacetate-derived amino acids: aspartate, asparagine, homoserine, isoleucine, lysine, and threonine.
C. reinhardtii was treated for 2 h with 5×10^{-9} mol L^{-1} IHg (IHg1), 5×10^{-8} mol L^{-1} IHg (IHg2), 5×10^{-9} mol L^{-1} MeHg (MeHg1), and 5×10^{-8} mol L^{-1} MeHg (MeHg2); the unexposed control (C).

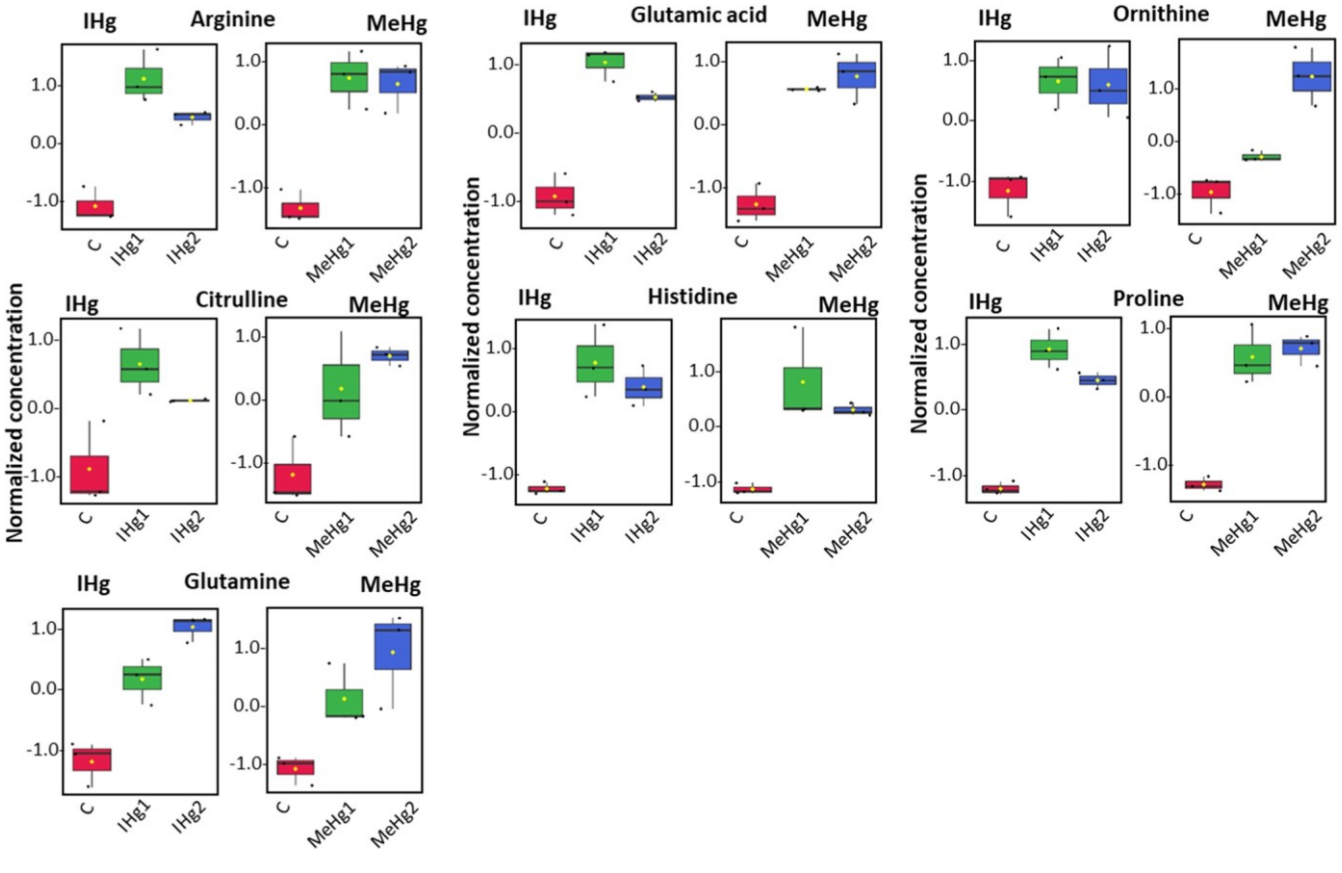

Figure 5. Box plots of relative abundance of α-ketoglutarate-derived amino acids: arginine, citrulline, glutamate, glutamine, ornithine, histidine, and proline. *C. reinhardtii* was treated for 2 h with 5×10^{-9} mol L^{-1} IHg (IHg1), 5×10^{-8} mol L^{-1} IHg (IHg2), 5×10^{-9} mol L^{-1} MeHg (MeHg1),and 5×10^{-8} mol L^{-1} MeHg (MeHg2); the unexposed control (C).

metabolites accumulated more strongly at lower Hg concen- trations (18 for IHg and 5 for MeHg). Group 2 included metabolites with comparable abundances at the two concen- trations (18 for IHg and 12 for MeHg, no concentration dependence). Group 3 encompassed metabolites accumulated

https://dx.doi.org/10.1021/acs.est.0c08416

to a larger degree at higher IHg or MeHg concentrations (8 for IHg ad 20 for MeHg).

The responsive metabolites identified by PLS-DA and ANOVA corresponded to 15 and 13 impacted pathways in IHg and MeHg treatments, respectively (Figures 3 and S4, Tables S4 and S5, impact threshold 0.1). The top five most

https://dx.doi.org/10.1021/acs.est.0c08416

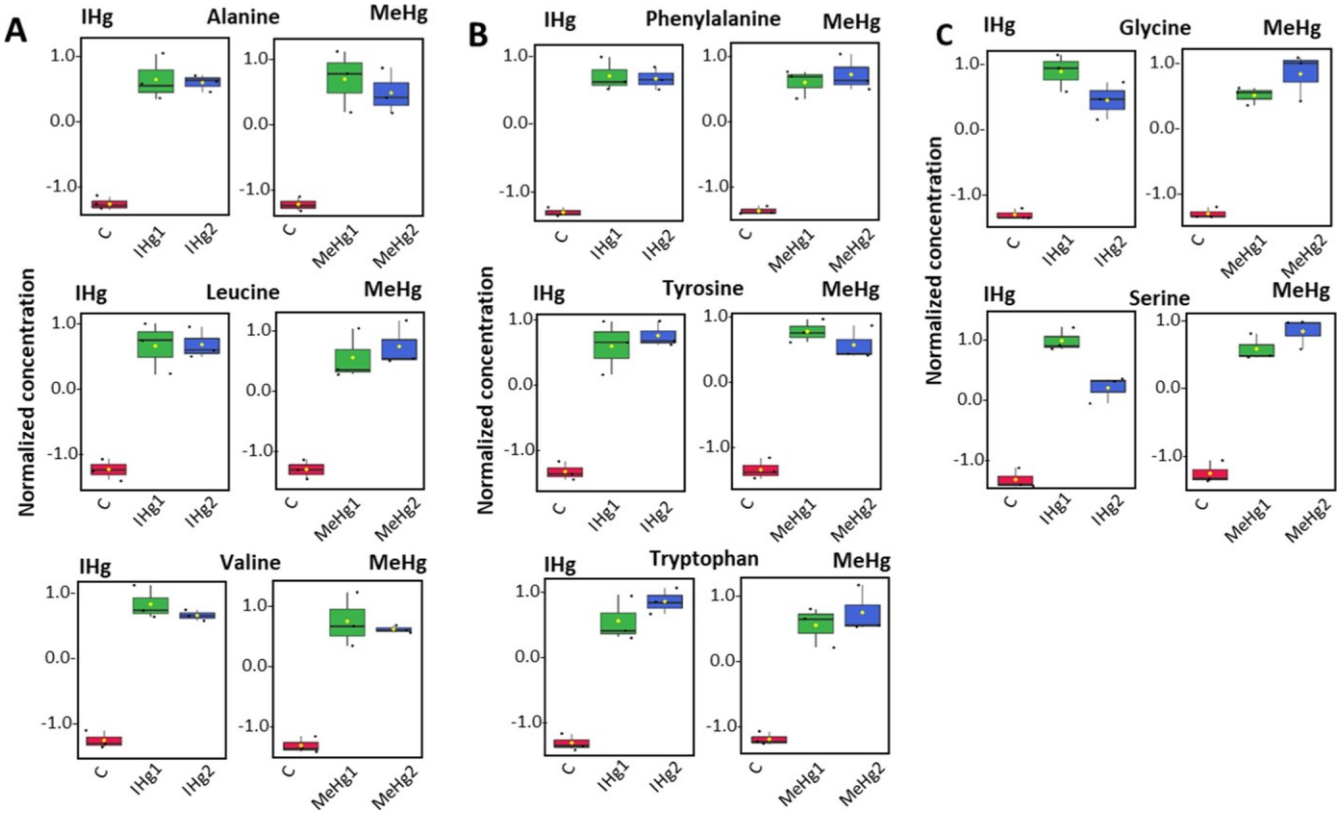

Figure 6. Box plots of relative abundance of (A) pyruvate-derived amino acid, alanine, leucine, and valine; (B) phosphoenolpyruvate-derived amino acids, phenylalanine, tyrosine, and tryptophan; and (C) glycine and serine. *C. reinhardtii* was treated for 2 h with 5×10^{-9} mol L^{-1} IHg (IHg1), 5×10^{-8} mol L^{-1} IHg (IHg2), 5×10^{-9} mol L^{-1} MeHg (MeHg1), and 5×10^{-8} mol L^{-1} MeHg (MeHg2); the unexposed control (C).

impacted pathways by sublethal concentrations of both IHg and MeHg included: (1) alanine, aspartate, and glutamate metabolism; (2) glycine, serine, and threonine metabolism; (3) arginine biosynthesis; (4) glutathione metabolism; and (5) isoquinoline alkaloid biosynthesis. These results confirmed the previous findings via transcriptomics that IHg and MeHg altered similar pathways in *C. reinhardtii*.[21,22] In addition, α- linolenic acid metabolism was significantly affected only by the IHg exposure (Table S4, Figure 3A).

Metabolic Perturbations in *C. reinhardtii* Exposed to Sublethal Levels of IHg and MeHg. *Amino Acid Metabolism*. Exposure to IHg and MeHg induced a significant dysregulation of the amino acid metabolism of *C. reinhardtii* (Figures 4–6). Amino acids represent structural units of the proteins and polypeptides, as well as serve as precursors for the synthesis of various metabolites with multiple functions in algal growth and other biological processes.[37−39] A significant increase ($p < 0.05$) in the relative abundance of 21 amino acids was observed in both IHg and MeHg treatments, implying an acceleration of the amino acid synthesis and/or degradation of proteins, as well as an active defense of *C. reinhardtii* from the stress induced by Hg compounds. As amino acids are part of the aminoacyl-tRNA biosynthesis, the increase in their abundance suggests that the exposure to both IHg and MeHg affects the synthesis of proteins that are central to algal growth. Similarly, the aminoacyl-tRNA biosynthesis in the aquatic plant *Elodea nuttallii* was affected by exposure to Cd and MeHg.[40]

Aspartate, generated by transamination of oxaloacetate, a tricarboxylic acid (TCA) cycle intermediate, accumulated in cells exposed to IHg and MeHg. *Aspartate* serves as a precursor

https://dx.doi.org/10.1021/acs.est.0c08416

for the biosynthesis of other amino acids: *asparagine, homoserine, threonine, lysine, and isoleucine*,[39] which were also accumulated (Figure 4). This finding is in line with our previous transcriptomics study,[22] showing that several genes driving the synthesis of amino acids were downregulated after exposure to IHg and MeHg [ASK1 coding for aspartate kinase; DPS1 gene for dihydrodipicolinate synthase, HSK1 for homoserine kinase (thrB1), and AAD1 for acetohydroxyacid dehydratase]. The ASNS gene that codes for asparagine synthase, which catalyzes amidation of aspartate to asparagine, was downregulated in the MeHg treatment.[22] The down-regulation of genes may be a compensatory response to the accumulation of amino acids. Indeed, metabolites not only are the final product of gene transcription but also can regulate gene transcription.

Glutamate, glutamine, ornithine, citrulline, arginine, and histidine biosynthesized from the TCA metabolite α- ketoglutarate[41] increased in cells exposed to both IHg and MeHg (Figure 5). Glutamine is part of the glutamine– glutamate cycle responsible for ammonia assimilation by *C. reinhardtii*.[39] The present findings are consistent with our previous transcriptomics results showing that genes GLN1, coding for glutamine synthetase, and GSF1, coding for ferredoxin-dependent glutamate synthase, were significantly upregulated in the MeHg treatment.[22] The assimilation of ammonia to glutamine and glutamate is catalyzed by the enzymes glutamine synthetase, glutamate synthase, and glutamate dehydrogenase. Glutamine synthetase also plays an important role in nitrate assimilation.[42] Therefore, these results suggest that assimilation of ammonia and nitrate is likely to be accelerated, supporting the finding that the levels of amino

https://dx.doi.org/10.1021/acs.est.0c08416

acids have been increased. In addition, gene GDH1, coding for the glutamate dehydrogenase 2, which catalyzes the trans- formation of glutamate to ammonium and α-ketoglutarate, was signi*fi*cantly downregulated in the MeHg treatment.[22]

The increase in the abundance of *histidine* observed in this study was consistent with signi*fi*cant downregulation of several genes coding for enzymes involved in di*ff*erent steps of the histidine biosynthesis, as observed in MeHg exposures in our previous study:[22] RPPK1-ribose-phosphate pyrophosphoki- nase; HDH1-histidinol dehydrogenase, and HIS3-imidazole- glycerol-phosphate dehydratase. Histidine is an amino acid needed for growth and development of algal cells, therefore the accumulation observed here reveals an in*fl*uence of Hg treatments on algal growth and cell development.

Proline plays an important role in osmo- and redox- regulation, metal chelation, and scavenging of free radicals induced by di*ff*erent metals including Hg in plants.[43,44] Proline accumulation in cells exposed to IHg and MeHg could be a defense response to oxidative stress and enable Hg complex- ation. As in plants, there are two alternative pathways in *C. reinhardtii* that are involved in the proline biosynthesis: the direct glutamate pathway and the ornithine pathway, where glutamate is *fi*rst converted to ornithine.[39] In our previous studies, PCR1 gene pyrroline-5-carboxylate reductase was upregulated in *C. reinhardtii* after exposure to MeHg.[22] The PCR1 gene encodes the enzyme Δ 1-pyrroline-5-carboxylate reductase, which controls the conversion of Δ 1-pyrroline-5- carboxylate to proline by the NADPH.[39]

Alanine, leucine, and valine are biosynthesized from pyruvate, a common metabolite of the intermediary metabolism.[39] They were signi*fi*cantly accumulated in Hg-exposed cells (Figure 6A). *Alanine* can be synthesized by reversible transamination of pyruvate with glutamate, which is catalyzed by alanine aminotransferase (AAT). The gene coding for AAT1 alanine aminotransferase is upregulated in IHg and MeHg treat- ments.[22] AAT is thought to play a role in photorespiration because of the ability of AAT to transaminate glyoxylate to glycine using glutamate as an amino donor.[39] Pyruvate also can be transaminated to alanine, a process catalyzed by alanine- glyoxylate aminotransferase (AGT1), but it is not considered to have a signi*fi*cant role in alanine synthesis.[39] Interestingly, the gene AGT1, coding for alanine-glyoxylate aminotransfer- ase, was upregulated signi*fi*cantly only in the MeHg treatment not in the IHg treatment. The gene BCA1 coding for branched-chain amino acid aminotransferase, involved in the biosynthesis of leucine from pyruvate, was upregulated in both IHg and MeHg treatments.[22] *Leucine* serves as an oxidative phosphorylation energy source.[45] The solely ketogenic amino acids, lysine, valine, and leucine, will be converted to acetyl- CoA and will presumably be used as a substrate for the TCA cycle or contribute to pools for fatty acid synthesis.[46] Using a *C. reinhardtii* mutant bkdE1α, it was shown that leucine, isoleucine, and valine, amino acids with a branched aliphatic chain, contribute to triacylglycerol metabolism by providing carbon precursors and ATP.[47] Indeed, leucine, isoleucine, and valine and their degradation products were shown to include acetyl-CoA, potential substrates for de novo fatty acid synthesis.[48]

Levels of aromatic amino acids, *phenylalanine, tyrosine, and tryptophan*, derived from phosphoenolpyruvate, were signi*fi*- cantly enhanced in Hg treatments (Figure 6B). Phenylalanine and tyrosine are precursors for the synthesis of pigments, including the carotenoids and PQ, respectively, via coumarate

https://dx.doi.org/10.1021/acs.est.0c08416

and acetoacetyl-CoA.[49] Carotenoids are bound to the protein complexes of the photosystem I and II of *C. reinhardtii* and known to protect the photosynthetic apparatus against photo- oxidative damage.[50] Therefore, the increased levels of phenyl- alanine and tyrosine suggest the acceleration of biosynthesis of carotenoids and enhanced cellular defense mechanisms. The accumulation of these amino acids concorded with the previously observed downregulation of multiple genes involved in their biosynthesis, in particularly in MeHg treatments.[22] For example, AGD1 gene coding for arogenate/prephenate dehydrogenase and PRD1 and TSA for tryptophan synthetase α-subunit were downregulated in MeHg exposure.[22]

Concentrations of two other amino acids, *glycine and serine*, were signi*fi*cantly increased by exposure to both IHg and MeHg (Figure 6C). Usually, these amino acids are synthesized by the photorespiratory glycolate cycle in algae,[39] so their accumulation could be interpreted as an acceleration of the photorespiratory activity, probably to produce the energy required for the synthesis of di*ff*erent defense components needed to cope with the stress induced by Hg treatments. This correlates well with the observed accumulation of glycolate (Figure S5), a photorespiratory intermediate. Photorespiration is one of the major carbon metabolism pathways in photosynthetic organisms;[51] therefore, the present results could indicate an acceleration of the C-metabolism of *C. reinhardtii* due to IHg and MeHg exposure. The possible acceleration of photorespiration is consistent with the upregulation in the MeHg treatment of the RbcS gene coding for ribulose-1,5-bisphosphate carboxylase/oxygenase, which catalyzes carbon *fi*xation to phosphoglycolate, and the PGP1 gene coding for phosphoglycolate phosphatase/4-nitrophenyl- phosphatase, involved in phosphoglycolate to glycolate conversion.[22] Possible acceleration of the photorespiratory glycolate cycle and the consequent increase of the serine concentration also corroborate with the upregulation of the SHMT1 and SGA1 genes after exposure to IHg and MeHg.[22] SGA1 coding for serine glyoxylate aminotransferase catalyzes the conversion of glyoxylate to glycine via serine. In addition, SHMT1 gene coding for serine hydroxymethyltransferase catalyzes the second step of the serine synthesized from two molecules of glycine in a two-step process via the glycine decarboxylase complex and serine hydroxymethyltransferase.[39] However, the ratios of glycine to serine, used as indicators of photorespiratory activity,[52] were comparable in IHg exposure (IHg1: 0.56 ± 0.04; IHg2: 0.63 ± 0.08), MeHg exposure (MeHg1: 0.55 ± 0.04; MeHg2: 0.57 ± 0.09), and in the unexposed control (C: 0.56 ± 0.10). Glycine and serine can also be synthesized by a non-photorespiratory pathway, the phosphorylated pathway,[39] which could probably be accel- erated. The phosphorylated serine pathway is catalyzed by the PGD1, PST1, and PSP1 enzymes; however, the gene coding for D-3-phosphoglycerate dehydrogenase (PGD1), for phosphoserine aminotransferase (PST1), and for phosphoserine phosphatase (PSP1) were not among the signi*fi*cantly dysregulated genes in IHg and MeHg exposure.[22] These *fi*ndings are in line with the increase in the maximum photosynthetic yield in MeHg treatments (Figure S6).

The accumulation of numerous amino acids could also contribute to chelation of Hg^{2+} and CH_3Hg^+ ions inside the cells.[44] The results from this study are consistent with the published studies demonstrating an accumulation of free amino acids in the green alga *Scenedesmus vacuolatus* exposed to prometryn,[53] *Chlorella vulgaris* to boscalid,[54] and *Dunaliella*

https://dx.doi.org/10.1021/acs.est.0c08416

tertiolecta to diuron.[55] Such an accumulation suggests alteration of the energy metabolism associated with the activation of catabolic processes and use of protein for the energy supply.[11] An increase in amino acid pools under stress conditions has been also reported in sulfur-depleted *C. reinhardtii* cells[56] and in *C. reinhardtii* under hyperosmotic stress.[57] However, the present findings for IHg and MeHg are opposite to the decrease of some of the amino acids (lysine, arginine, and glutamine) observed in copper exposure of other green algae *Chlorella* sp.,[58,59] *Scenedesmus quadricauda,*[60] and diatom *Tabellaria flocculosa* (Roth) Kützing.[61]

Nucleobase/-Tide/-Side Metabolism. The metabolism of both pyrimidine and purine derivatives was significantly affected in algae exposed to IHg and MeHg (Figures S7 and S8). The *pyrimidine* nucleobases, *cytosine* and *uracil*, signifi- cantly increased, as well as the corresponding nucleotides/- sides, cytidine monophosphate (*CMP*) and *uridine*. Interest- ingly, the levels of these metabolites were greater at lower IHg concentrations (IHg1) than at higher exposure (IHg2), whereas in the MeHg exposure, their relative abundance increased with the exposure concentration. The above observation is consistent with the increase of glutamine and aspartate, amino acids used for biosynthesis of uridine monophosphate and CMP nucleotides. The thymidine mono- phosphate metabolism seems unaffected by Hg-treatments. Pyrimidine nucleotides are involved in the synthesis of glycogen and phospholipids, which seems to accelerate due to exposure to mercury.[62] CMP accumulation is consistent with upregulation, for MeHg treatments, of the genes coding for CDP-ethanolamine: DAG ethanolamine phosphotransfer- ase, which catalyzes the conversion of CDP-choline and 1,2-diacylglycerol to CMP and α phosphatidylcholine.[22]

The *purine* metabolites (*AMP*, *adenosine*, *adenine*, *hypoxan- thine*, *xanthine*, *guanosine,* and *guanine*) significantly accumu- lated in algae exposed to both IHg and MeHg as compared with unexposed controls (Figure S8). However, their abundances increased with the exposure concentration only for MeHg. No significant changes in the abundance of other nucleobases/-tides/-sides such as IMP, GMP, and inosine were observed. Such nucleobase accumulation after Hg treatments could be related to an acceleration of their synthesis, a respective nucleoside/nucleotide degradation, and salvaged for reincorporation into nucleotides. Indeed, the DNA and RNA could be hydrolyzed by nucleases to yield a mixture of polynucleotides, which are transformed to mononucleotides. They are further converted by the nucleosidases to nucleo- sides, which undergo phosphorolysis to yield the nucleobase. In our previous study, FAP215 gene coding for nucleotidase and flagellar-associated protein was downregulated in both IHg and MeHg treatments,[22] in agreement with the accumulated nucleosides (adenosine, guanosine, and hypoxanthine).

The above results indicate a significant upregulation of the pyrimidine and purine metabolism of *C. reinhardtii* by exposure to sublethal IHg and MeHg concentrations. Pyrimidine and purine nucleotides are structural units of the nucleic acids DNA and RNA.[62] Therefore, the present results suggest an acceleration of DNA and RNA synthesis and turnover. They are in good agreement with the amino acid upregulation as the amino acids serve as precursors for a wide variety of metabolites including purine and pyrimidine nucleotides.[39]

Antioxidant Metabolism. Exposure to both IHg and MeHg led to a significant increase of *reduced glutathione (GSH)* after Hg treatments (Figure S5). Since GSH is central to redox

https://dx.doi.org/10.1021/acs.est.0c08416

control in the cell,[63] this finding suggests an activation of the defense mechanism against the oxidative stress due to exposure to IHg and MeHg. GSH acts as a redox buffer for the protection of cells against the reactive oxygen species (ROS) produced by Hg.[17] Indeed, no significant generation of the ROS or membrane damage was found in *C. reinhardtii* exposed to IHg and MeHg (Figure S6). GHS is a precursor of phytochelatin [(−Glu−Cys)$_n$−Gly with n = 2−11, PCn] synthesis, which is activated by different toxic metals including Hg.[64] PCns are considered major intracellular chelators for Hg detoxification.[17] GSH is also an important metal chelator in plant cells and may also contribute to Hg detoxification.[65] Indeed, GSH is an important thiol involved in Hg sequestration in green algae.[66] However, exposure to IHg resulted in a significant decline in GSH cellular concentrations in other green algae, such as *Cosmarium conspersum* and *Chlorella autotrophica*;[67] it may reflect consumption of GSH after the interaction with ROS. In this study, for a comparable exposure concentration, IHg induced a significant depletion of GSH in comparison with MeHg, suggesting higher potency of IHg to induce PCn than that of MeHg. This is in line with the existing literature, showing formation of IHg−PCn complexes in green algae[68] and lower PCn induction capability of MeHg in the diatom cells.[69] GHS concentration in *C. reinhardtii* decreased during exposure to Cu,[70,71] whereas Cd exposure increased GHS concentrations as an antioxidant response by cells.[71,72] The increase in GSH observed here is consistent with the previously observed upregulation of genes coding for glutathione peroxidase, an enzyme catalyzing the formation of glutathione disulfide (GS-SG) for GSH, in MeHg (GPX3) and IHg (GPX5) treatments.[22]

Ascorbic acid accumulated in *C. reinhardtii* cells after IHg and MeHg treatments. Ascorbic acid is a cellular antioxidant, and it is involved in different cellular processes associated with photosynthetic functions and stress tolerance.[73] Increased concentrations of ascorbate could also play a role in preservation of the GSH pool and maintenance of the cellular redox balance by forming a primary barrier to ROS.[73] The accumulation of ascorbic acid showed that the antioxidant defense system of *C. reinhardtii* was activated by the IHg and MeHg treatments. Ascorbic acid is also known to play an important role in plant cell photoprotection.[74]

Contrary to this finding, exposure to 10^{-4} mol L^{-1} IHg concentrations depleted ascorbic acid in the green alga *Coccomyxa subellipsoidea*;[75] however, the concentrations of IHg were 2×10^3 to 2×10^4 times higher than those used in the present study. Micromolar concentrations of IHg are known to induce a rapid increase in ROS in the alga *Chlamydomonas* at micromolar doses.[17,76] However, for IHg and MeHg concentrations comparable with those in the present work, no significant oxidative stress in *C. reinhardtii* was observed.[22,77] The above results suggest that the algal cells limit ROS enhancement through an efficient antioxidant response at the metabolic level, well before the effects are observed physiologically.

Carboxylic Acid Metabolism. Three of the TCA intermediates (citric, succinic, and malic acids) were significantly increased after IHg treatment (Figure S5). The effect was more pronounced in IHg treatments since for the MeHg treatments, only the level of succinic acid was significantly enhanced. The changes in concentrations of citric and malic acids after MeHg treatment were not statistically significant (p > 0.05) (Figure S5). Similar to that in IHg

https://dx.doi.org/10.1021/acs.est.0c08416

exposure, the concentrations of citric, succinic, and malic acids increased significantly in *Poterioochromonas malhamensis* exposed to Ag and AgNPs,[13] as well as the level of malic acid in *Scenedesmus obliquus* exposed to AgNPs.[78] By contrast, a decrease in the TCA intermediates was observed in the diatom *T. flocculosa* exposed to high Cu concentrations.[79] As the TCA cycle is the core of the cell's respiratory machinery, it is likely that the increase in TCA intermediates observed here could be related to an increase in energy production necessary for the manufacture of defense compounds needed to cope with Hg-induced stress. The above findings are consistent with the observed alteration of genes involved in the TCA cycle.[22] Gene IDH3, coding for NAD-dependent isocitrate dehydrogenase and NADP-dependent isocitrate dehydrogenase, which catalyzes the first carbon oxidation in the TCA cycle (i.e., oxaloacetate → 2-oxoglutarate), were downregulated by MeHg but not by IHg. The succinate-to-fumarate conversion is catalyzed by the succinate dehydrogenase; succinate dehydro- genase 1-1 and succinate dehydrogenase were both strongly downregulated by MeHg, whereas only succinate dehydrogen- ase 1-1 was downregulated in IHg treatments. MDH1 NAD- dependent malate dehydrogenase was downregulated by both IHg and MeHg treatments, whereas MDH2 NADP- dependent malate dehydrogenase, chloroplastic was upregu- lated in IHg and MeHg treatments. Malate dehydrogenase is part of the second carbon oxidation and catalyzes the conversion of 2-oxoglutarate to oxaloacetate.

Carbohydrate Metabolism. Of the 13 carbohydrates that were analyzed, only three were above detection limits and quantified: glucose/galactose, sucrose, and maltose. Only the increase in abundance of maltose was statistically significant ($p > 0.05$) in cells treated with IHg or MeHg. *Maltose* is produced from starch and similar compounds in plants and can be further hydrolyzed to glucose by the enzyme maltase.[80] Maltose metabolism in plants is considered to make a "bridge between transitory starch breakdown and the plants' adaptation to changes in environmental conditions".[81] Micro- algae store fixed carbon as starch in their chloroplasts. As needed, starch is converted to maltose and exported from the chloroplast to the cytosol, where maltose is converted to glucose, used as an energy source.[82] This suggests that algae exposed to IHg or MeHg experience impaired carbohydrate biosynthesis. Accumulation of maltose and no changes in the glucose abundance suggest that conversion of starch to maltose was accelerated as an energy supply. This last suggestion is consistent with the upregulation of the MEX1 gene coding for maltose exporter-like protein, MEX1, which was shown to be essential for starch degradation in *C. reinhardtii*.[83] Similarly, AMYA1 α-amylase-like 3 gene was upregulated in *C. reinhardtii* by exposure to a comparable concentration of MeHg.[22] Taken together with the alteration of the amino acid metabolism, TCA cycle, and carbohydrates, this finding suggests the activation of catabolic processes to restore energy balance incells exposed to Hg compounds.

Fatty Acid Metabolism. Among the eight fatty acids considered, two saturated acids [i.e., *palmitic* (hexadecanoic acid, 16:0) and *stearic* (octadecanoic acid, 18:0) acids] and two unsaturated acids [i.e., *linolenic* (C 9,12,15 double bonds) and *linoleic* (C 9,12 double bonds) acids] accumulated in cells exposed to IHg (Figure S9). After MeHg exposure, only palmitic acid increased significantly, whereas the changes in the abundance of linoleic acid, linolenic acid, and stearic acid were not significantly different from that in the unexposed control

https://dx.doi.org/10.1021/acs.est.0c08416

(all $p > 0.05$). Similar changes in fatty acid composition have been frequently observed in algae under toxic metal stress.[84] Exposure to Cu resulted in an increase in the concentration of palmitic acid in *T. flocculosa*.[79] AgNPs and dissolved Ag induced an accumulation of linolenic acid, whereas arachidic and stearic acids were depleted in *P. malhamensis*.[13] Exposure to AgNPs and $AgNO_3$ reduced the abundance of mono-unsaturated and polyunsaturated fatty acids of the green microalga *C. vulgaris*.[85] The results suggest that algae exposed to IHg, and in a lower degree to MeHg, remodel the membrane *fl*uidity to make it more tolerant to oxidation, thus preserving membrane integrity under oxidative stress con- ditions.[86] Indeed, palmitic acid is known to be less prone to oxidation than other fatty acids.[86] A perturbation of the metabolism of fatty acids could also change the cellular energy budget.[87]

An increase in *ethanolamine* abundance was only observed in the IHg exposure, indicating alteration of the glycerophospho- lipid biosynthesis pathway by IHg. As glycerophospholipids are the main component of cell membranes, a decrease of those compounds can compromise membrane integrity. Opposite to the present *fi*nding, a decrease in ethanolamine was observed in other phytoplankton species such as *Chlorella* sp. exposed to copper.[58]

Overall, the present targeted metabolomics study provides for the *fi*rst time information on the metabolic perturbations in the green alga *C. reinhardtii* exposed to sublethal concen- trations of IHg and MeHg and thus serves to improve biological understanding of the molecular basis of these perturbations. The results revealed that during exposure to IHg and MeHg the alga accumulates metabolites involved in various metabolic pathways corresponding to amino acid and nucleotide synthesis and degradation, fatty acids, carbohy- drates, TCA, antioxidants, and photorespiration. Most of the observed metabolic perturbations were observed in both IHg and MeHg treatments. However, the exposure to IHg induced more pronounced perturbations in fatty acid and TCA metabolism than the exposure to MeHg. The observed metabolic perturbations were generally consistent with previous transcriptomics results for *C. reinhardtii* exposed to IHg and MeHg. The results show that metabolites respond faster to IHg and MeHg exposure than algal physiology and demonstrate the potential of metabolomics for toxicity evaluation, especially to identify biochemical markers and to detect e*ff*ects at low toxicant levels and an early stage of exposure.

ASSOCIATED CONTENT

Supporting Information

The Supporting Information is available free of charge at https://pubs.acs.org/doi/10.1021/acs.est.0c08416.

Cellular mercury content in the alga *C. reinhardtii*; VIP scores from PLS-DA analysis of discriminating metab- olites between unexposed controls and IHg treatments; VIP scores from PLS-DA analysis of discriminating metabolites between unexposed controls and MeHg treatments; metabolic pathways from KEGG with at least two signi*fi*cantly dysregulated metabolites by IHg or MeHg exposure; box plots of relative abundance of metabolites involved in carboxylic acid metabolism and antioxidants; e*ff*ect of IHg and MeHg exposure on physiology of *C. reinhardtii*, including membrane

https://dx.doi.org/10.1021/acs.est.0c08416

damage assessed by PI stain and flow cytometry (FCM), ROS generation determined by CellRxOX Green stain and FCM, chlorophyll *a*, and maximum quantum yield of photosystem II (F_v/F_m); box plots of relative abundance of nucleobases/-tides/-sides of pyrimidine metabolism; box plots of relative abundance of nucleobases/-tides/-sides of purine metabolism; box plots of relative abundance of metabolites involved in fatty acid metabolism and ethanolamine; measured metabolites and the MS parameters for LC–MS targeted metabolomics; important features identified by one-way ANOVA and Fisher's post-hoc analysis ($p < 0.05$) in *C. reinhardtii* exposed to 5×10^{-9} mol L^{-1} IHg (MeHg1) and 5×10^{-8} mol L^{-1} IHg (MeHg2); important features identified by one-way ANOVA and Fisher's post-hoc analysis ($p < 0.05$) in *C. reinhardtii* exposed to 5×10^{-9} mol L^{-1} MeHg (MeHg1) and 5×10^{-8} mol L^{-1} MeHg (MeHg2); and pathways analysis for IHg exposure MeHg exposure (PDF)

AUTHOR INFORMATION

Corresponding Author

Vera I. Slaveykova – *Faculty of Sciences, Earth and Environment Sciences, Department F.-A. Forel for Environmental and Aquatic Sciences, Environmental Biogeochemistry and Ecotoxicology, University of Geneva, Geneva CH 1211, Switzerland;* orcid.org/0000-0002-8361-2509; Email: vera.slaveykova@unige.ch

Authors

Sanghamitra Majumdar – *Bren School of Environmental Science & Management, University of California, Santa Barbara, Santa Barbara, California 93106-5131, United States*

Nicole Regier – *Faculty of Sciences, Earth and Environment Sciences, Department F.-A. Forel for Environmental andAquatic Sciences, Environmental Biogeochemistry and Ecotoxicology, University of Geneva, Geneva CH 1211, Switzerland*

Weiwei Li – *Bren School of Environmental Science & Management, University of California, Santa Barbara, SantaBarbara, California 93106-5131, United States*

Arturo A. Keller – *Bren School of Environmental Science & Management, University of California, Santa Barbara, SantaBarbara, California 93106-5131, United States;* orcid.org/0000-0002-7638-662X

Complete contact information is available at: https://pubs.acs.org/10.1021/acs.est.0c08416

Author Contributions

V.I.S. and A.A.K. conceived and designed the study. N.R. performed exposure bioassays and measured Hg in the exposure medium and algae. W.L. performed the LC–MS measurements, S.M. prepared the samples for metabolomics and overviewed the LC–MS measurements, and V.I.S. performed the analysis and interpretation of metabolomic results, wrote the manuscript, and overviewed the overall study. A.A.K. took part in the data interpretation and manuscript writing and overviewed the overall study. All the authors critically commented on and revised the manuscript. All the authors have approved the paper submission.

https://dx.doi.org/10.1021/acs.est.0c08416

Notes

The authors declare no competing financial interest.

ACKNOWLEDGMENTS

V.I.S. acknowledges the financial support of the Swiss National Science Foundation (grant IZSEZ0_180186). A.A.K. acknowl- edges the support of the U.S. National Science Foundation (grant NSF 1901515). Any opinions, findings, and conclusions or recommendations expressed in this material are those of the author(s) and do not necessarily reflect the views of the funding agencies.

REFERENCES

(1) Sturla, S. J.; Boobis, A. R.; FitzGerald, R. E.; Hoeng, J.; Kavlock, R. J.; Schirmer, K.; Whelan, M.; Wilks, M. F.; Peitsch, M. C. Systems Toxicology: From Basic Research to Risk Assessment. *Chem. Res. Toxicol.* 2014, *27*, 314–329.

(2) Zhang, X.; Xia, P.; Wang, P.; Yang, J.; Baird, D. J. Omics Advances in Ecotoxicology. *Environ. Sci. Technol.* 2018, *52*, 3842– 3851.

(3) Fiehn, O. Metabolomics the link between genotypes and phenotypes. *Plant Mol. Biol.* 2002, *48*, 155–171.

(4) Patti, G. J.; Yanes, O.; Siuzdak, G. Metabolomics: the apogee of the omics trilogy. *Nat. Rev. Mol. Cell Biol.* 2012, *13*, 263–269.

(5) Johnson, C. H.; Ivanisevic, J.; Siuzdak, G. Metabolomics: beyond biomarkers and towards mechanisms. *Nat. Rev. Mol. Cell Biol.* 2016,*17*, 451–459.

(6) Mangal, V.; Nguyen, T. Q.; Fiering, Q.; Guéguen, C. An untargeted metabolomic approach for the putative characterization of metabolites from Scenedesmus obliquus in response to cadmium stress. *Environ. Pollut.* 2020, *266*, 115123.

(7) Samuelsson, L. M.; Larsson, D. G. J. Contributions from metabolomics to fish research. *Mol. BioSyst.* 2008, *4*, 974–979.

(8) Viant, M. R. Recent developments in environmental metabolomics. *Mol. BioSyst.* 2008, *4*, 980–986.

(9) Matich, E. K.; Chavez Soria, N. G.; Aga, D. S.; Atilla-Gokcumen, G. E. Applications of metabolomics in assessing ecological effects of emerging contaminants and pollutants on plants. *J. Hazard. Mater.* 2019, *373*, 527–535.

(10) Majumdar, S.; Keller, A. A. Omics to address the opportunities and challenges of nanotechnology in agriculture. *Crit. Rev. Environ. Sci. Technol.* 2020, 1–42.

(11) Gauthier, L.; Tison-Rosebery, J.; Morin, S.; Mazzella, N. Metabolome response to anthropogenic contamination on micro- algae: a review. *Metabolomics* 2020, *16*, 8.

(12) Huang, M.; Keller, A. A.; Wang, X.; Tian, L.; Wu, B.; Ji, R.; Zhao, L. Low Concentrations of Silver Nanoparticles and Silver Ions Perturb the Antioxidant Defense System and Nitrogen Metabolism in N2-Fixing Cyanobacteria. *Environ. Sci. Technol.* 2020, *54*, 15996– 16005.

(13) Liu, W.; Majumdar, S.; Li, W.; Keller, A. A.; Slaveykova, V. I. Metabolomics for early detection of stress in freshwater alga *Poterioochromonas malhamensis* exposed to silver nanoparticles. *Sci. Rep.* 2020, *10*, 20563.

(14) Driscoll, C. T.; Mason, R. P.; Chan, H. M.; Jacob, D. J.; Pirrone, N. Mercury as a Global Pollutant: Sources, Pathways, and Effects. *Environ. Sci. Technol.* 2013, *47*, 4967–4983.

(15) Sakamoto, M.; Murata, K.; Kakita, A.; Sasaki, M. A Review of Mercury Toxicity with Special Reference to Methylmercury. In *Environmental Chemistry and Toxicology of Mercury*; Liu, G., Cai, Y., O'Driscoll, N., Eds.; John Wiley & Sons, 2011; pp 501–516.

(16) Yang, L.; Zhang, Y.; Wang, F.; Luo, Z.; Guo, S.; Strähle, U. Toxicity of mercury: Molecular evidence. *Chemosphere* 2020, *245*, 125586.

(17) Le Faucheur, S.; Campbell, P. G. C.; Fortin, C.; Slaveykova, V. I. Interactions between mercury and phytoplankton: Speciation, bioavailability, and internal handling. *Environ. Toxicol. Chem.* 2014, *33*, 1211–1224.

https://dx.doi.org/10.1021/acs.est.0c08416

(18) Dranguet, P.; Flück, R.; Regier, N.; Cosio, C.; Le Faucheur, S.; Slaveykova, V. I. Towards Mechanistic Understanding of Mercury Availability and Toxicity to Aquatic Primary Producers. *Chimia* 2014, *68*, 799–805.

(19) Cosio, C.; Flück, R.; Regier, N.; Slaveykova, V. I. Effects of
macrophytes on the fate of mercury in aquatic systems. *Environ. Toxicol. Chem.* 2014, *33*, 1225–1237.

(20) Beauvais-Flück, R.; Slaveykova, V.; Cosio, C. Molecular Effects of Inorganic and Methyl Mercury in Aquatic Primary Producers: Comparing Impact to A Macrophyte and A Green Microalga in Controlled Conditions. *Geosciences* 2018, *8*, 393.

(21) Beauvais-Flück, R.; Slaveykova, V. I.; Cosio, C. Transcriptomic
and physiological responses of the green microalga Chlamydomonas reinhardtii during short-term exposure to subnanomolar methylmer- cury concentrations. *Environ. Sci. Technol.* 2016, *50*, 7126–7134.

(22) Beauvais-Flück, R.; Slaveykova, V. I.; Cosio, C. Cellular toxicity
pathways of inorganic and methyl mercury in the green microalga Chlamydomonas reinhardtii. *Sci. Rep.* 2017, *7*, 8034.

(23) Dranguet, P.; Cosio, C.; Le Faucheur, S.; Beauvais-Flück, R.;
Freiburghaus, A.; Worms, I. A. M.; Petit, B.; Civic, N.; Docquier, M.; Slaveykova, V. I. Transcriptomic approach for assessment of the impact on microalga and macrophyte of in-situ exposure in river sites contaminated by chlor-alkali plant effluents. *Water Res.* 2017, *121*, 86–94.

(24) Fernie, A. R.; Stitt, M. On the Discordance of Metabolomics with Proteomics and Transcriptomics: Coping with Increasing Complexity in Logic, Chemistry, and Network Interactions Scientific Correspondence. *Plant Physiol.* 2012, *158*, 1139–1145.

(25) Cajka, T.; Fiehn, O. Toward Merging Untargeted and Targeted Methods in Mass Spectrometry-Based Metabolomics and Lipidomics. *Anal. Chem.* 2016, *88*, 524–545.

(26) Harris, E. H. *The Chlamydomonas Sourcebook: A Comprehensive Guide to Biology and Laboratory Use*; Elsevier, 2013.

(27) Puzanskiy, R.; Tarakhovskaya, E.; Shavarda, A.; Shishova, M. Metabolomic and physiological changes of Chlamydomonas rein- hardtii (Chlorophyceae, Chlorophyta) during batch culture develop- ment. *J. Appl. Phycol.* 2018, *30*, 803–818.

(28) Davis, M. C.; Fiehn, O.; Durnford, D. G. Metabolic acclimation to excess light intensity in Chlamydomonas reinhardtii. *Plant, Cell Environ.* 2013, *36*, 1391–1405.

(29) Huang, Y.; Li, W.; Minakova, A. S.; Anumol, T.; Keller, A. A. Quantitative analysis of changes in amino acids levels for cucumber (Cucumis sativus) exposed to nano copper. *NanoImpact* 2018, *12*, 9– 17.

(30) Huang, Y.; Adeleye, A. S.; Zhao, L.; Minakova, A. S.; Anumol, T.; Keller, A. A. Antioxidant response of cucumber (Cucumis sativus) exposed to nano copper pesticide: Quantitative determination via LC- MS/MS. *Food Chem.* 2019, *270*, 47–52.

(31) Majumdar, S.; Pagano, L.; Wohlschlegel, J. A.; Villani, M.; Zappettini, A.; White, J. C.; Keller, A. A. Proteomic, gene and metabolite characterization reveal the uptake and toxicity mechanisms of cadmium sulfide quantum dots in soybean plants. *Environ. Sci.: Nano* 2019, *6*, 3010–3026.

(32) Xia, J.; Wishart, D. S. Web-based inference of biological patterns, functions and pathways from metabolomic data using MetaboAnalyst. *Nat. Protoc.* 2011, *6*, 743.

(33) Chong, J.; Wishart, D. S.; Xia, J. Using MetaboAnalyst 4.0 for Comprehensive and Integrative Metabolomics Data Analysis. *Curr. Protoc. Bioinf.* 2019, *68*, No. e86.

(34) Johnson, W. E.; Li, C.; Rabinovic, A. Adjusting batch effects in microarray expression data using empirical Bayes methods. *Biosta- tistics* 2006, *8*, 118–127.

(35) Jung, Y.; Ahn, Y. G.; Kim, H. K.; Moon, B. C.; Lee, A. Y.; Ryu,
D. H.; Hwang, G.-S. Characterization of dandelion species using 1H NMR- and GC-MS-based metabolite profiling. *Analyst* 2011, *136*, 4222–4231.

(36) Xia, J.; Wishart, D. S. MSEA: a web-based tool to identify biologically meaningful patterns in quantitative metabolomic data. *Nucleic Acids Res.* 2010, *38*, W71–W77.

https://dx.doi.org/10.1021/acs.est.0c08416

(37) Bromke, M. Amino Acid Biosynthesis Pathways in Diatoms. *Metabolites* 2013, *3*, 294–311.
(38) Hildebrandt, T. M.; Nunes Nesi, A.; Araújo, W. L.; Braun, H.-P. Amino Acid Catabolism in Plants. *Mol. Plant* 2015, *8*, 1563–1579.
(39) Vallon, O.; Spalding, M. H. Amino Acid Metabolism. In *The Chlamydomonas Sourcebook*, 2nd ed.; Harris, E. H., Stern, D. B., Witman, G. B., Eds.; Academic Press: London, 2009; Chapter 4, pp 115–158.
(40) Cosio, C.; Renault, D. Effects of cadmium, inorganic mercury and methyl-mercury on the physiology and metabolomic profiles of shoots of the macrophyte Elodea nuttallii. *Environ. Pollut.* 2020, *257*, 113557.
(41) Less, H.; Galili, G. Principal Transcriptional Programs Regulating Plant Amino Acid Metabolism in Response to Abiotic Stresses. *Plant Physiol.* 2008, *147*, 316–330.
(42) Cullimore, J. V.; Sims, A. P. Glutamine synthetase of Chlamydomonas: its role in the control of nitrate assimilation. *Planta* 1981, *153*, 18–24.
(43) Matysik, J.; Alia; Bhalu, B.; Mohanty, P. Molecular mechanisms of quenching of reactive oxygen species by proline under stress in plants. *Curr. Sci.* 2002, *82*, 525–532.
(44) Sharma, S. S.; Dietz, K.-J. The significance of amino acids and amino acid-derived molecules in plant responses and adaptation to heavy metal stress. *J. Exp. Bot.* 2006, *57*, 711–726.
(45) Taylor, N. L.; Heazlewood, J. L.; Day, D. A.; Millar, A. H. Lipoic acid-dependent oxidative catabolism of alpha-keto acids in mitochondria provides evidence for branched-chain amino acid catabolism in Arabidopsis. *Plant Physiol.* 2004, *134*, 838–848.
(46) Johnson, X.; Alric, J. Central Carbon Metabolism and Electron Transport in Chlamydomonas reinhardtii: Metabolic Constraints for Carbon Partitioning between Oil and Starch. *Eukaryotic Cell* 2013, *12*, 776–793.
(47) Liang, Y.; Kong, F.; Torres-Romero, I.; Burlacot, A.; Cuine, S.; Légeret, B.; Billon, E.; Brotman, Y.; Alseekh, S.; Fernie, A. R.; Beisson, F.; Peltier, G.; Li-Beisson, Y. Branched-Chain Amino Acid Catabolism Impacts Triacylglycerol Homeostasis in Chlamydomonas reinhardtii. *Plant Physiol.* 2019, *179*, 1502–1514.
(48) Binder, S.; Knill, T.; Schuster, J. Branched-chain amino acid metabolism in higher plants. *Physiol. Plant.* 2007, *129*, 68–78.
(49) Antonacci, A.; Lambreva, M. D.; Margonelli, A.; Sobolev, A. P.; Pastorelli, S.; Bertalan, I.; Johanningmeier, U.; Sobolev, V.; Samish, I.; Edelman, M.; Havurinne, V.; Tyystjärvi, E.; Giardi, M. T.; Mattoo, A. K.; Rea, G. Photosystem-II D1 protein mutants of Chlamydomonas reinhardtii in relation to metabolic rewiring and remodelling of H- bond network at QB site. *Sci. Rep.* 2018, *8*, 14745.
(50) Lohr, M. Carotenoids. In *The Chlamydomonas Sourcebook*, 2nd ed.; Harris, E. H., Stern, D. B., Witman, G. B., Eds.; Academic Press: London, 2009; Chapter 21, pp 799–817.
(51) Dellero, Y.; Jossier, M.; Schmitz, J.; Maurino, V. G.; Hodges, M. Photorespiratory glycolate–glyoxylate metabolism. *J. Exp. Bot.* 2016, *67*, 3041–3052.
(52) Timm, S.; Florian, A.; Wittmiß, M.; Jahnke, K.; Hagemann, M.; Fernie, A. R.; Bauwe, H. Serine acts as a metabolic signal for the transcriptional control of photorespiration-related genes in Arabi- dopsis. *Plant Physiol.* 2013, *162*, 379–389.
(53) Kluender, C.; Sans-Piché, F.; Riedl, J.; Altenburger, R.; Härtig, C.; Laue, G.; Schmitt-Jansen, M. A metabolomics approach to assessing phytotoxic effects on the green alga Scenedesmus vacuolatus. *Metabolomics* 2008, *5*, 59.
(54) Qian, L.; Qi, S.; Cao, F.; Zhang, J.; Zhao, F.; Li, C.; Wang, C. Toxic effects of boscalid on the growth, photosynthesis, antioxidant system and metabolism of Chlorella vulgaris. *Environ. Pollut.* 2018, *242*, 171–181.
(55) Booij, P.; Lamoree, M. H.; Sjollema, S. B.; Voogt, P. d.; Schollee, J. E.; Vethaak, A. D.; Leonards, P. E. G. Non-target Metabolomic Profiling of the Marine Microalgae *Dunaliella tertiolecta* After Exposure to Diuron using Complementary High- Resolution Analytical Techniques. *Curr. Metabolomics* 2014, *2*, 213–222.

https://dx.doi.org/10.1021/acs.est.0c08416

(56) Matthew, T.; Zhou, W.; Rupprecht, J.; Lim, L.; Thomas-Hall, S. R.; Doebbe, A.; Kruse, O.; Hankamer, B.; Marx, U. C.; Smith, S. M.; Schenk, P. M. The metabolome of Chlamydomonas reinhardtii following induction of anaerobic H2 production by sulfur depletion. *J. Biol. Chem.* 2009, *284*, 23415−23425.

(57) Tietel, Z.; Wikoff, W. R.; Kind, T.; Ma, Y.; Fiehn, O.
Hyperosmotic stress in Chlamydomonas induces metabolomic changes in biosynthesis of complex lipids. *Eur. J. Phycol.* 2020, *55*, 11−29.

(58) Zhang, W.; Tan, N. G. J.; Fu, B.; Li, S. F. Y. Metallomics and NMR-based metabolomics of Chlorella sp. reveal the synergistic role of copper and cadmium in multi-metal toxicity and oxidative stress. *Metallomics* 2015, *7*, 426−438.

(59) Zhang, W.; Tan, N. G. J.; Li, S. F. Y. NMR-based metabolomics and LC-MS/MS quantification reveal metal-specific tolerance and redox homeostasis in Chlorella vulgaris. *Mol. BioSyst.* 2014, *10*, 149− 160.

(60) Yong, W.-K.; Sim, K.-S.; Poong, S.-W.; Wei, D.; Phang, S.-M.; Lim, P.-E. Interactive effects of temperature and copper toxicity on photosynthetic efficiency and metabolic plasticity in Scenedesmus quadricauda (Chlorophyceae). *J. Appl. Phycol.* 2018, *30*, 3029−3041.

(61) Gonçalves, S.; Kahlert, M.; Almeida, S. F. P.; Figueira, E.
Assessing Cu impacts on freshwater diatoms: biochemical and metabolomic responses of Tabellaria flocculosa (Roth) Kützing. *Sci. Total Environ.* 2018, *625*, 1234−1246.

(62) Bhagavan, N. V.; Ha, C.-E. Nucleotide Metabolism. In *Essentials of Medical Biochemistry*; Ha, N. V. B. C.-E., Ed.; Academic Press, 2015; Chapter 25, p 752.

(63) Foyer, C. H.; Noctor, G. Ascorbate and Glutathione: The Heart of the Redox Hub. *Plant Physiol.* 2011, *155*, 2−18.

(64) Grill, E.; Löffler, S.; Winnacker, E.-L.; Zenk, M. H. Phytochelatins, the heavy-metal-binding peptides of plants, are synthesized from glutathione by a specific γ-glutamylcysteine dipeptidyl transpeptidase (phytochelatin synthase). *Proc. Natl. Acad. Sci. U.S.A.* 1989, *86*, 6838−6842.

(65) Jozefczak, M.; Remans, T.; Vangronsveld, J.; Cuypers, A. Glutathione is a key player in metal-induced oxidative stress defenses. *Int. J. Mol. Sci.* 2012, *13*, 3145−3175.

(66) Agrawal, S. B.; Agrawal, M.; Lee, E. H.; Kramer, G. F.; Pillai, P. Changes in polyamine and glutathione contents of a green alga, Chlorogonium elongatum (Dang) France exposed to mercury. *Environ. Exp. Bot.* 1992, *32*, 145−151.

(67) Wu, Y.; Wang, W.-X. Intracellular speciation and transformation of inorganic mercury in marine phytoplankton. *Aquat. Toxicol.* 2014, *148*, 122−129.

(68) Gómez-Jacinto, V.; García-Barrera, T.; Gómez-Ariza, J. L.; Garbayo-Nores, I.; Vílchez-Lobato, C. Elucidation of the defence mechanism in microalgae Chlorella sorokiniana under mercury exposure. Identification of Hg−phytochelatins. *Chem.-Biol. Interact.* 2015, *238*, 82−90.

(69) Wu, Y.; Wang, W.-X. Thiol compounds induction kinetics in marine phytoplankton during and after mercury exposure. *J. Hazard. Mater.* 2012, *217*, 271−278.

(70) Jamers, A.; Blust, R.; De Coen, W.; Griffin, J. L.; Jones, O. A. Copper toxicity in the microalga Chlamydomonas reinhardtii: an integrated approach. *BioMetals* 2013, *26*, 731.

(71) Stoiber, T. L.; Shafer, M. M.; Armstrong, D. E. Differential effects of copper and cadmium exposure on toxicity endpoints and gene expression in Chlamydomonas reinhardtii. *Environ. Toxicol.Chem.* 2010, *29*, 191−200.

(72) Jamers, A.; Blust, R.; De Coen, W.; Griffin, J. L.; Jones, O. A. H. An omics based assessment of cadmium toxicity in the green alga Chlamydomonas reinhardtii. *Aquat. Toxicol.* 2013, *126*, 355−364.

(73) Gest, N.; Gautier, H.; Stevens, R. Ascorbate as seen through plant evolution: the rise of a successful molecule? *J. Exp. Bot.* 2012, *64*, 33−53.

(74) Smirnoff, N. Ascorbic acid: metabolism and functions of a multi-facetted molecule. *Curr. Opin. Plant Biol.* 2000, *3*, 229−235.

https://dx.doi.org/10.1021/acs.est.0c08416

(75) Kovácík, J.; Rotkova, G.; Bujdos, M.; Babula, P.; Peterkova, V.; Matus, P. Ascorbic acid protects Coccomyxa subellipsoidea against metal toxicity through modulation of ROS/NO balance and metal uptake. *J. Hazard. Mater.* 2017, *339*, 200−207.

(76) Elbaz, A.; Wei, Y. Y.; Meng, Q.; Zheng, Q.; Yang, Z. M. Mercury-induced oxidative stress and impact on antioxidant enzymes in Chlamydomonas reinhardtii. *Ecotoxicology* 2010, *19*, 1285−1293.

(77) Beauvais-Flück, R.; Slaveykova, V. I.; Cosio, C. Transcriptomic and Physiological Responses of the Green Microalga Chlamydomonas reinhardtii during Short-Term Exposure to Subnanomolar Methyl- mercury Concentrations. *Environ. Sci. Technol.* 2016, *50*, 7126−7134.

(78) Wang, P.; Zhang, B.; Zhang, H.; He, Y.; Ong, C. N.; Yang, J. Metabolites change of Scenedesmus obliquus exerted by AgNPs. *J. Environ. Sci.* 2019, *76*, 310−318.

(79) Gonçalves, S.; Kahlert, M.; Almeida, S. F. P.; Figueira, E. Assessing Cu impacts on freshwater diatoms: biochemical and metabolomic responses of Tabellaria flocculosa (Roth) Kutzing. *Sci. Total Environ.* 2018, *625*, 1234−1246.

(80) Weise, S. E.; Weber, A. P. M.; Sharkey, T. D. Maltose is the major form of carbon exported from the chloroplast at night. *Planta* 2004, *218*, 474−482.

(81) Lu, Y.; Sharkey, T. D. The importance of maltose in transitory starch breakdown. *Plant, Cell Environ.* 2006, *29*, 353−366.

(82) Hostettler, C.; Kölling, K.; Santelia, D.; Streb, S.; Kötting, O.; Zeeman, S. C. Analysis of starch metabolism in chloroplasts. *Methods Mol. Biol.* 2011, *775*, 387−410.

(83) Findinier, J.; Tuncay, H.; Schulz-Raffelt, M.; Deschamps, P.; Spriet, C.; Lacroix, J.-M.; Duchêne, T.; Szydlowski, N.; Li-Beisson, Y.; Peltier, G.; D'Hulst, C.; Wattebled, F.; Dauvillée, D. The Chlamydomonas mex1 mutant shows impaired starch mobilization without maltose accumulation. *J. Exp. Bot.* 2017, *68*, 5177−5189.

(84) Pinto, E.; Sigaud-kutner, T. C. S.; Leitão M. A. S.; Okamoto, O. K.; Morse, D.; Colepicolo, P. Heavy metal-induced ooxidative stress in algae. *J. Phycol.* 2003, *39*, 1008−1018.

(85) Behzadi Tayemeh, M.; Esmailbeigi, M.; Shirdel, I.; Joo, H. S.; Johari, S. A.; Banan, A.; Nourani, H.; Mashhadi, H.; Jami, M. J.; Tabarrok, M. Perturbation of fatty acid composition, pigments, and growth indices of Chlorella vulgaris in response to silver ions and nanoparticles: A new holistic understanding of hidden ecotoxico- logical aspect of pollutants. *Chemosphere* 2020, *238*, 124576.

(86) Upchurch, R. G. Fatty acid unsaturation, mobilization, and regulation in the response of plants to stress. *Biotechnol. Lett.* 2008, *30*, 967−977.

(87) Filimonova, V.; Gonçalves, F.; Marques, J. C.; De Troch, M.; Gonçalves, A. M. M. Fatty acid profiling as bioindicator of chemical stress in marine organisms: A review. *Ecol. Indic.* 2016, *67*, 657−672.

https://dx.doi.org/10.1021/acs.est.0c08416